Aimon K. Alkanani,[1] Naoko Hara,[1] Egil Lien,[2] Diana Ir,[3] Cassandra V. Kotter,[3] Charles E. Robertson,[4,5] Brandie D. Wagner,[5,6] Daniel N. Frank,[3,5] and Danny Zipris[1]

Induction of Diabetes in the RIP-B7.1 Mouse Model Is Critically Dependent on TLR3 and MyD88 Pathways and Is Associated With Alterations in the Intestinal Microbiome

RIP-B7.1 transgenic mice express B7.1 costimulatory molecules in pancreatic islets and develop diabetes after treatment with polyinosinic: polycytidylic acid (poly I:C), a synthetic double-stranded RNA and agonist of Toll-like receptor (TLR) 3 and retinoic acid–inducible protein I. We used this model to investigate the role of TLR pathways and intestinal microbiota in disease progression. RIP-B7.1 mice homozygous for targeted disruption of TLR9, TLR3, and myeloid differentiation factor-88 (MyD88), and most of the wild-type RIP-B7.1 mice housed under normal conditions remained diabetes-free after poly I:C administration. However, the majority of TLR9-deficient mice and wild-type animals treated with poly I:C and an antibiotic developed disease. In sharp contrast, TLR3- and MyD88-deficient mice were protected from diabetes following the same treatment regimen. High-throughput DNA sequencing demonstrated that TLR9-deficient mice treated with antibiotics plus poly I:C had higher bacterial diversity compared with disease-resistant mice. Furthermore, principal component analysis suggested that TLR9-deficient mice had distinct gut microbiome compared with the diabetes-resistant mice. Finally, the administration of sulfatrim plus poly I:C to TLR9-deficient mice resulted in alterations in the abundance of gut bacterial communities at the phylum and genus levels. These data imply that the induction of diabetes in the RIP-B7.1 model is critically dependent on TLR3 and MyD88 pathways, and involves modulation of the intestinal microbiota.

Diabetes 2014;63:619–631 | DOI: 10.2337/db13-1007

Type 1 diabetes (T1D) is a proinflammatory autoimmune disease that involves the specific destruction of pancreatic β-cells (1). The etiology of the disease is incompletely

[1]Barbara Davis Center for Childhood Diabetes, University of Colorado Denver, Aurora, CO
[2]Department of Medicine, Division of Infectious Diseases and Immunology, University of Massachusetts Medical School, Worcester, MA
[3]Division of Infectious Diseases, University of Colorado School of Medicine, Aurora, CO
[4]Department of Molecular, Cellular, and Developmental Biology, University of Colorado, Boulder, CO
[5]University of Colorado Microbiome Research Consortium, Aurora, CO
[6]Department of Biostatistics and Informatics, Colorado School of Public Health, University of Colorado Denver, Aurora, CO
Corresponding author: Danny Zipris, danny.zipris@ucdenver.edu.

Received 27 June 2013 and accepted 7 October 2013.
This article contains Supplementary Data online at http://diabetes.diabetesjournals.org/lookup/suppl/doi:10.2337/db13-1007/-/DC1.

understood; however, epidemiological data and evidence from animal models of T1D implicate microbes in the disease course (2).

The innate immune system uses pattern-recognition receptors, such as Toll-like receptors (TLRs), nucleotide-binding oligomerization domain (NOD)-like receptors, and retinoic acid–inducible gene-1 (RIG-I)–like receptors, to detect and eradicate microbial infections (3). Interactions between TLRs and their ligands initiate a series of intracellular signaling events leading to the expression of antimicrobial genes, proinflammatory cytokines, and chemokines, such as type I interferons, interleukin (IL)-1, IL-6, IL-12, and chemokine (C-X-C motif) ligand-10 (3,4). Emerging evidence has implicated the innate immune system and TLR pathways in the mechanism of T1D (reviewed in Chervonsky [5], Wong and Wen [6], and Zipris [7]).

The gut microbiota play a central role in shaping the peripheral and intestinal immune systems in health and disease (5,8–10). The gut microbiome has recently been implicated in chronic proinflammatory disorders, including T1D (11–18). A temporal decline in members of the bacterial phyla Firmicutes and an increase in Bacteroidetes has been observed in individuals that are at risk for developing T1D, compared with healthy subjects (13). Other investigators have shown that intestinal bacteria are associated with T1D in the diabetes-prone BioBreeding rat (19), the LEW1.WR1 rat model of virus-induced T1D (20), and the NOD mouse (14,21).

The RIP-B7.1 transgenic mouse expresses B7.1 costimulatory molecules under the control of the rat insulin promoter (22). The administration of double-stranded RNA, a ligand of TLR3 and RIG-like helicases, in these animals results in diabetes via mechanisms that have been hypothesized to involve type I interferon pathways (23) and the upregulation of antigen-presenting cells and T-cell auto-reactivity (24). In the current study, we used the RIP-B7.1 mouse model of diabetes to investigate the role of TLR pathways and the intestinal microbiota in the mechanism of disease induction. We demonstrate that the TLR3 and myeloid differentiation factor-88 (MyD88) pathways, but not the TLR9 pathway, play a critical role in the mechanism of islet destruction. Furthermore, we provide evidence that alterations in the gut microbiota may be involved in the course of polyinosinic:polycytidylic acid (poly I:C)–induced diabetes in this animal model.

RESEARCH DESIGN AND METHODS

Mice

C57BL/6 mice with pancreatic β-cells expressing B7.1 costimulatory molecules under the rat insulin promoter (RIP-B7.1) were produced as previously described (22) and bred in the University of Colorado animal facility. To generate RIP-B7.1 mice deficient in TLR9, TLR3, or MyD88, RIP-B7.1 mice were bred to homozygosity with C57BL/6 mice deficient in TLR9, TLR3, or MyD88 (25). The B7.1 transgene expression and/or gene mutation were detected by PCR amplification using genomic DNA isolated from tail snips (22). All animals were housed in a specific pathogen-free facility and maintained in accordance with the Guide for the Care and Use of Laboratory Animals (published by the National Institutes of Health, NIH publication no. 86-23, revised 1996) and the guidelines of the Institutional Animal Care and Use Committee of the University of Colorado Denver.

TLR Activation, Antibiotic Treatment, Blood Removal, and Serum p40 Measurements

To induce diabetes, mice at 6–8 weeks of age were injected intraperitoneally with 5 μg/g body weight poly I:C (Sigma-Aldrich, St. Louis, MO) on 10 consecutive days. Mice were given normal water or water supplemented with sulfatrim (1 mg/mL sulfamethoxazole plus 0.2 mg/mL trimethoprim; Hi-Tech Pharmacal, Amityville, NY) beginning at birth and continuing for the duration of the experiment. Animals were monitored for disease development for at least 200 days after poly I:C treatment. Blood glucose was measured twice a week, and the mice were considered diabetic after two consecutive blood glucose test results of >250 mg/dL. To investigate the expression of the p40 subunit of IL-12 and IL-23, mice received 5 μg/g body weight of poly I:C or CpG DNA (TriLink BioTechnologies). Blood was collected 6 h after the treatment. Sera were separated from blood cells immediately after blood collection and stored at −80°C until use. The serum level of the p40 subunit of IL-12 and IL-23 was measured using a commercial kit from Life Technologies-Invitrogen (Carlsbad, CA) according to the manufacturer's instructions.

DNA Isolation and Quantitative RT-PCR Analysis for the Detection of Gut Bacteria

The *Lactobacillus*, *Bifidobacterium*, *Clostridium*, and *Bacteroides* genera were detected in stool DNA by quantitative PCR analysis using previously published primers (26). Bacterial DNA was recovered from stool using the QIAmp DNA stool mini kit (Qiagen, Valencia, CA) according to the manufacturer's instructions. DNA concentrations were determined using a NanoDrop ND-1000 spectrophotometer (Thermo Scientific, Wilmington, DE). The data were normalized to the total bacterial DNA in each sample using previously described primers and conditions (26).

High-Throughput DNA Sequencing for Microbiome Analysis

16S Amplicon Library Construction

Bacterial profiles from the mice were determined by broad-range amplification and sequence analysis of 16S ribosomal RNA (rRNA) genes following our previously described methods (20,27). In brief, amplicons were generated using primers that target approximately 300 base pairs of the V4 variable region of the 16S rRNA gene. PCR products were normalized using a SequalPrep

kit (Invitrogen), and were pooled, lyophilized, purified, and concentrated using a DNA Clean and Concentrator Kit (Zymo, Irvine, CA). Pooled amplicons was quantified using Qubit Fluorometer 2.0 (Invitrogen). The pool was diluted to 2 nmol/L and denatured with 0.2N NaOH at room temperature. The denatured DNA was diluted to 15 pmol/L and spiked with 25% of the Illumina PhiX control DNA prior to loading the sequencer. Illumina paired-end sequencing was performed on the Miseq platform with version 2.0 of the Miseq Control Software, using a 500-cycle version 2 reagent kit.

Analysis of Illumina Paired-End Reads

Illumina Miseq paired-end sequences were sorted by sample via barcodes in the paired reads with a python script. The sorted, paired reads were assembled using phrap (28). Assembled sequence ends were trimmed over a moving window of 5 nucleotides until average quality met or exceeded 20. Trimmed sequences with more than one ambiguity or shorter than 200 nucleotides were discarded. Potential chimeras identified with Uchime (usearch6.0.203_i86linux32) (29) using the Schloss and Westcott (30) Silva reference sequences were removed from subsequent analyses. Assembled sequences were aligned and classified with SINA (1.2.11) (31) using the 244,077 bacterial sequences in Silva 111NR (32), as reference configured to yield the Silva taxonomy. Operational taxonomic units (OTUs) were produced by clustering sequences with identical taxonomic assignments. The software package Explicet (33) was used for display, analysis, and figure generation of results. The median goods coverage score for libraries, a measure of the completeness of sequencing, was ≥99%, indicating that the depth of sequencing was sufficient to fully describe the biodiversity of the samples.

Bioinformatics and Statistical Analysis

Statistical comparisons of diabetes-free survival among groups were performed using the Kaplan-Meier method. Comparisons between more than two groups were performed using a one-way ANOVA with Bonferroni multiple-comparison test. Comparisons between two groups were performed with the unpaired *t* test.

Ecological indices of richness (e.g., S_{obs}, S_{chao}), diversity (e.g., Shannon's diversity [H_o] and evenness [H_o/H_{max}]), and coverage (e.g., Good's index) were calculated with Explicet (33) and compared across groups with an ANOVA. These indices were estimated through bootstrap resampling (1,000 replicates) and rarefaction of the OTU distributions obtained from each specimen. For ease of interpretation, effective number of species was calculated (34). These values represent the expected number of taxa in an even community. Two-part tests were used to perform pairwise comparisons across groups separately for each OTU (20). Because of the exploratory nature of this study, *P* values were not corrected for multiple tests, as we have recently published (20). To investigate the data multivariately (across genera), a principal component analysis (PCA) was performed using singular value decomposition of the centered data using the prcomp function in R. A small constant (1/total number of sequences) was added to the counts prior to the application of the centered log ratio transformation recommended for compositional data (35,36).

RESULTS

Poly I:C–Induced Diabetes in RIP-B7.1 Mice with Disrupted TLR Signaling

TLR pathways have been suggested to play a key role in the mechanism leading to diabetes in humans and in an animal model (5,6,37,38). We sought to test this hypothesis in the C57BL/6 transgenic RIP-B7.1 mouse. Islet β-cells in this mouse express B7.1 molecules, leading to diabetes after intraperitoneal administration of poly I:C (24), which binds TLR3 as well as TLR-independent RNA helicases, such as RIG-I and melanoma differentiation-associated protein-5 (39). To determine the roles of TLR receptors in diabetes pathogenesis, C57BL/6 mice homozygous for disrupted TLR signaling pathways were bred to RIP-B7.1 mice to homozygosity, resulting in RIP-B7.1 mice deficient in TLR9, TLR3, or MyD88. Mice of 6–8 weeks of age were injected intraperitoneally with 5 μg/g body weight poly I:C on 10 consecutive days and monitored for diabetes for at least 200 days after the last poly I:C injection. The data shown in Fig. 1*A* demonstrate that only 8% of wild-type RIP-B7.1 mice housed under normal conditions and treated with poly I:C developed disease (n = 12). In addition, none of the mice deficient in TLR9, TLR3, or MyD88 expression developed diabetes after poly I:C administration (Fig. 1*B* and data not shown; n = 5–10 per group).

Given the potential role of intestinal bacteria in the development of T1D (14), we investigated the possibility that modulating the gut microbiome with an antibiotic treatment could affect the course of diabetes in the RIP-B7.1 model. To that end, mice were treated with sulfatrim in the drinking water beginning at birth and were injected with 5 μg/g body weight poly I:C at 6–8 weeks of age on 10 consecutive days. In contrast to mice receiving normal water, 90% of the wild-type RIP-B7.1 mice treated with poly I:C plus sulfatrim developed diabetes (n = 10, P = 0.0001 vs. mice receiving normal water). Furthermore, all of the RIP-B7.1 mice deficient in TLR9 developed diabetes after the administration of sulfatrim plus poly I:C (Fig. 1*B*; n = 11, $P < 0.0001$ vs. mice receiving normal water) with a more rapid disease progression compared with similarly treated RIP-B7.1 wild-type mice ($P < 0.01$). However, none of the TLR3- or MyD88-deficient RIP-B7.1 mice (n = 9 per group) developed hyperglycemia following the same treatment regimen ($P < 0.0001$ vs. TLR9-deficient RIP-B7.1 mice). Finally, mice that received sulfatrim in the absence of poly I:C did not develop diabetes (data not shown). Taken together, our observations suggest that TLR3 and MyD88 pathways, but not the TLR9 pathway, are

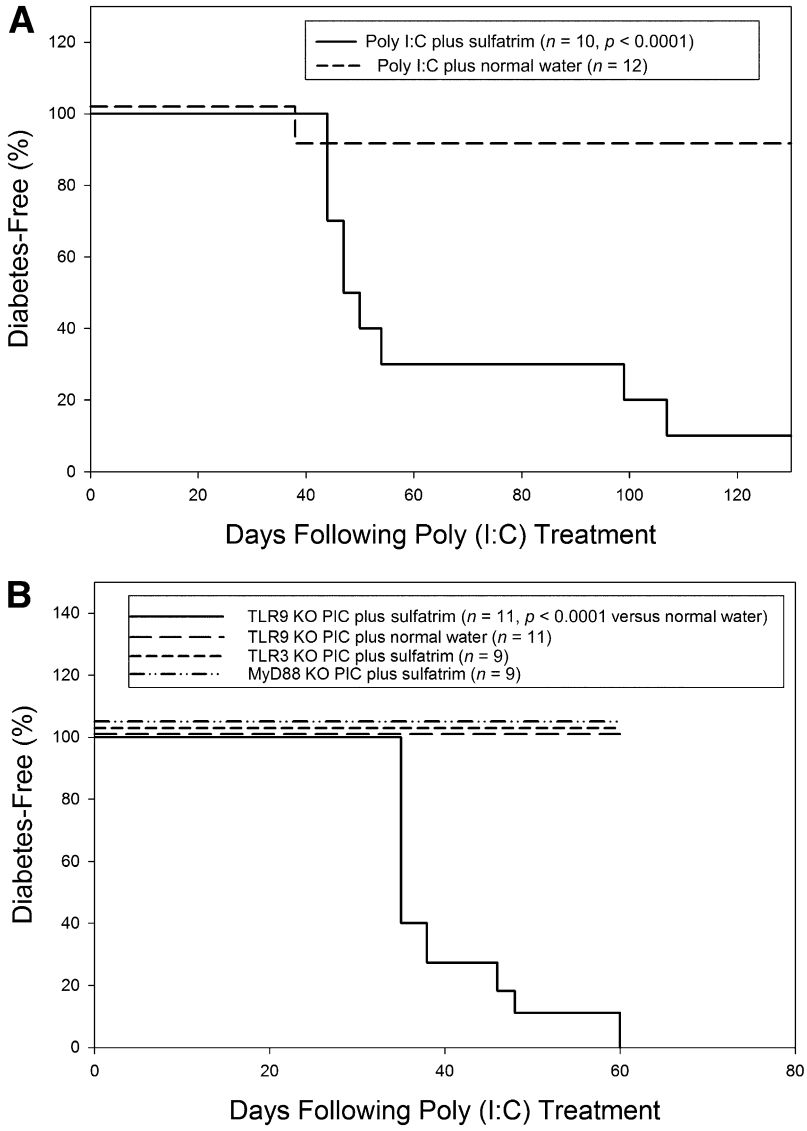

Figure 1—Kaplan-Meier analysis of poly I:C–induced diabetes in RIP-B7.1 mice. RIP-B7.1 with intact (*A*) and disrupted TLR signaling (*B*) of either sex were given normal drinking water or water supplemented with sulfatrim beginning at birth, as indicated. Animals at 6–8 weeks of age were injected intraperitoneally with 5 μg/g body weight poly I:C for 10 consecutive days. The animals were tested for disease development for at least 200 days after the last poly I:C injection. Disease was defined as the presence of plasma glucose concentrations >250 mg/dL (11.1 mmol/L) for 2 consecutive days. Survival was analyzed using the Kaplan-Meier method. Statistical analyses among groups were performed using the log-rank test. KO, knockout; PIC, poly I:C.

absolutely required for disease development and that intestinal bacteria play a central role in regulating the anti-islet autoimmune process in the RIP-B7.1 model. The data also suggest that the TLR9 pathway may play a regulatory role in disease development.

TLR9-Deficient RIP-B7.1 Mice Treated With Sulfatrim Plus Poly I:C Have Gut Microbiomes With Higher Bacterial Diversity

Because we observed that TLR9-deficient RIP-B7.1 mice developed diabetes after sulfatrim treatment, we postulated that disease mechanisms might involve alterations in gut bacterial communities. To test this hypothesis, we used broad-range PCR amplification and sequencing of bacterial 16*S* rRNA gene V4 variable regions to analyze fecal samples from TLR9-deficient versus TLR3- and MyD88-deficient mice.

Mice were provided *1*) normal water, *2*) poly I:C only, *3*) sulfatrim only, or *4*) sulfatrim plus poly I:C (n = 3–10 mice per group). Given the fact that poly I:C, but not lipopolysaccharide (LPS), induces diabetes in TLR9-deficient RIP-B7.1 mice (Fig. 1 and data not shown) and to better understand the role of the intestinal microbiota in diabetes development in TLR9-deficient animals, we analyzed the effects of LPS and poly I:C on the intestinal microbiota. To that end, groups of mice were treated with LPS or poly I:C on 10 consecutive days, and fecal samples were collected on day 5 after the last injection.

We compared between the gut microbiome of diabetes-susceptible TLR9-deficient mice treated with a regimen that promotes disease development (sulfatrim plus poly I:C versus a regimen that does not induce diabetes [sulfatrim plus LPS]). We also analyzed the effects of disease promoting regimen on the intestinal microbiota of diabetes-susceptible (TLR9-deficient) versus diabetes-resistant (MyD88 and TLR3-deficient) strains. A median of 131,000 sequences (range 60,000 to 334,000 sequences) were obtained for each sample, and overall 158 different bacterial genera were identified (Table 1 and Table 2 and data not shown).

To examine whether diabetes is linked to altered microbiota, we first assessed community diversity by calculating Shannon indices based on the 16*S* rDNA sequences in each sample. No significant differences in the bacterial diversity were noted between diabetes-susceptible and disease-resistant mice that received water only (Fig. 2). Increased bacterial diversity, however, was observed in TLR9-deficient mice treated with sulfatrim plus poly I:C with a twofold increase in the effective number of genera compared with all other groups (18.2 vs. 9.2, $P < 0.01$). Using pairwise comparisons, we found that the mean Shannon diversity in TLR9-deficient mice treated with sulfatrim plus poly I:C was significantly higher and slightly increased compared with sulfatrim plus poly I:C-treated TLR3- and MyD88-deficient mice, respectively ($P = 0.0002$ and $P = 0.06$, respectively). Finally, a significant difference in diversity was observed in TLR9-deficient mice that received sulfatrim plus poly I:C compared with sulfatrim plus LPS ($P < 0.01$). These findings suggest that treatment with sulfatrim plus poly I:C alters the composition of the microbiome, resulting in higher bacterial diversity in TLR9-deficient compared with diabetes-resistant mice.

Altered Gut Microbiomes of TLR9-Deficient Mice Treated With Sulfatrim Plus Poly I:C Compared With Diabetes-Resistant Mice

We used PCA to identify differences in the distributions of bacterial genera from animals that received treatment with antibiotics and TLR ligands (Fig. 3). The majority of the TLR9-deficient mice treated with the diabetes-inducing agents sulfatrim plus poly I:C and those mice that received water or sulfatrim only, treatment regimens that do not lead to disease onset, clustered together at a position that was distinct from the other mouse strains and had gut microbiota composed of higher levels of *Mucispirillum*, *Leuconostoc*, and *Lactococcus*, and lower abundance of Porphyromonadaceae, *Rikenella*, *Marvinbryantia*, and Desulfovibrionaceae. Interestingly, all five TLR9-deficient mice that received sulfatrim plus LPS, a treatment regimen that does not lead to diabetes, clustered together with the diabetes-resistant TLR3- and MyD88-deficient mice, and had reduced levels of *Mucispirillum*, *Leuconostoc*, and *Lactococcus*. These data suggest that poly I:C plus sulfatrim–induced islet destruction may be associated with intestinal microbiota that are distinct from those induced by LPS plus sulfatrim in mice with TLR9 deficiency, or those induced by poly I:C plus sulfatrim in diabetes-resistant TLR3–deficient and MyD88–deficient RIP-B7.1 mice.

TLR9-Deficient Mice Have Alterations in the Abundance of Gut Bacterial Communities

Comparable numbers of genera were detected (i.e., genus richness) in treated compared with untreated animals. Table 1 and Table 2 show that the administration of sulfatrim plus poly I:C induced a significant increase in the relative abundance of the phylum Actinobacteria in TLR9- versus MyD88-deficient mice (4.2 vs. 0.09%, $P < 0.05$). Within the Actinobacteria, there was a 50-fold increase in the level of the *Bifidobacterium* genus in mice deficient in TLR9 versus MyD88 (3.37 vs. 0.07, respectively; $P < 0.05$). No such differences were evident in fecal samples from TLR9-deficient compared with TLR3- and MyD88-deficient RIP-B7.1 mice that received poly I:C without antibiotics (Supplementary Table 1). TLR9-deficient mice had reduced abundance of Bacteroidetes compared with MyD88-deficient mice ($P < 0.1$). Most notable in this bacterial phylum was a reduction in the level of Porphyromonadaceae, RC9-gut-group, and *Rikenella* seen in TLR9- versus MyD88-deficient mice ($P < 0.01$ for all bacteria). An increase and a reduction in the abundance of Actinobacteria and Bacteroidetes, respectively, were observed in the stool from TLR9- versus TLR3-deficient mice after the administration of sulfatrim plus poly I:C; however, these differences did not reach a statistically significant level, probably due to the smaller number of animals included in the TLR3-deficient mouse group.

To further investigate the potential role of the intestinal microbiome in disease development, we compared the gut microbiome in mice given sulfatrim plus poly I:C versus sulfatrim plus LPS. The latter treatment regimen does not induce diabetes (24) (data not shown). Table 1 indicates that TLR9-deficient mice administered sulfatrim plus LPS had 40- to 50-fold lower levels of the *Bifidobacterium* genus and Cyanobacteria phylum, most notably in the *4C0-d2* genus ($P < 0.05$ vs. sulfatrim plus poly I:C). Furthermore, a reduction and an increase in the abundance of Firmicutes and Bacteroidetes, respectively, were found in mice injected with LPS compared with poly I:C. Together, the data lend further support to the hypothesis that disease induction is associated with altered gut bacterial composition in TLR9-deficient mice.

Validation of High-Throughput Sequencing Data

We used quantitative PCR to validate the high-throughput sequencing data and to further investigate the intestinal microbiome at the genus level. Animals were given sulfatrim only ($n = 4$–8) or sulfatrim plus poly I:C ($n = 5$–8) for 10 consecutive days. We evaluated the abundance of the bacterial genera *Bifidobacterium*, *Clostridium*, *Lactobacillus*,

Table 1—Percentage prevalence and median abundance of bacterial phyla and genera in RIP-B7.1 mice with disrupted TLR3 and TLR9 signaling

	TLR3						TLR9					
	Sulfatrim		Sulfatrim plus LPS[b]		Sulfatrim plus PIC		Sulfatrim		Sulfatrim plus LPS		Sulfatrim plus PIC	
Taxonomy[a]	Prevalence[c]	Abundance[d]	Prevalence[c]	Abundance[d]	Prevalence[c]	Abundance[d]	Prevalence[c]	Abundance[d]	Prevalence[c]	Abundance[d]	Prevalence[c]	Abundance[d]
Actinobacteria	100	2.80	100	0.26	100	0.09	100	0.09	100	0.13	100	4.17
Bifidobacterium	100	0.14	100	0.16	100	0.08	100	0.07	100	**0.06**[e,*]	100	3.37
Coriobacteriaceae	100	0.01	100	0.08	83	0.00	100	0.01	10	**0.05**	100	0.04
Enterorhabdus	100	0.03	100	0.01	100	0.01	100	0.03	100	**0.04**	100	0.13
Bacteroidetes	100	57.23	100	69.63	100	72.45	100	56.63	100	**73.77****	100	53.3
Alistipes	100	0.34	100	2.72	100	0.37	100	2.99	100	**0.97***	100	6.22
Bacteroidales	83	0.01	100	0.07	100	0.04	100	0.06	100	**0.09***	100	0.05
Bacteroides	100	0.79	100	1.84	100	2.82	100	1.88	100	2.33	100	2.22
Parabacteroides	100	0.01	100	0.09	100	0.04	100	0.87	100	**0.12***	100	0.49
Porphyromonadaceae	100	0.03	100	0.16	100	**0.34*****	67	0.06	80	**0.00**	33	0.03
RC9-gut-group	100	0.10	100	1.6	100	**0.47*****	100	0.64	100	0.42	67	0.00
Rikenella	100	0.09	50	0.00	67	0.09	67	0.06	100	0.06	0.5	0.00
S24–7	100	54.56	100	59.77	100	62.44	100	46.73	100	**67.15***	100	42.9
Cyanobacteria	100	0.02	50	0.01	100	0.14	100	0.12	100	**0.01***	83	0.37
4C0d-2	100	0.02	50	0.00	100	0.14	100	0.12	100	**0.01***	83	0.36
Firmicutes	100	38.79	100	12.95	100	16.53	100	35.30	100	**12.50***	100	36.8
Anaerotruncus	100	0.20	100	0.06	100	0.13	100	0.36	100	**0.09****	100	0.22
Christensenellaceae	83	0.00	50	0.00	50	0.00	100	0.00	100	**0.03***	100	0.00
Clostridiales	100	1.25	100	1.25	100	2.37	100	1.05	100	**0.63****	100	2.98
Coprococcus	100	0.16	100	0.02	100	0.04	100	0.09	100	**0.16***	100	0.08
Erysipelotrichaceae	100	0.04	100	0.17	100	0.06	100	0.53	100	**0.42***	100	0.06
Sequences/specimen[f]	69,409		123,099		145,310		268,824		137,452		225,364	
Good's coverage (%)	99.99		99.99		99.99		99.99		99.99		99.99	
Genus richness	42.5		44.5		42.5		51.0		45.0		44.5	
Samples (*n*)	6		2		6		3		5		6	

The numbers in bold represent differences with P values <0.01, <0.05, or <0.1. PIC, poly I:C. [a]Phylogeny of bacterial taxa, assigned by 16S rRNA sequence analysis. [b]The LPS data from the TLR3- and MyD88-deficient RIP-B7.1 mice were also included for reference but were excluded from statistical analysis. [c]Prevalence (%) of 16S rRNA sequences for bacterial clade and treatment group. [d]Median relative abundance (%) of 16S rRNA sequences for bacterial clade and treatment group. [e]Results of a two-part statistical test of bacterial prevalence and abundance. [f]Median values. *$P < 0.05$, **$P < 0.1$, comparison of TLR9-deficient mice treated with sulfatrim plus PIC vs. sulfatrim plus LPS. ***$P < 0.1$, comparison of TLR3-deficient mice treated with sulfatrim vs. sulfatrim plus PIC.

Table 2—Percentage prevalence and median abundance of bacterial phyla and genera in RIP-B7.1 mice deficient of MyD88

	Sulfatrim		Sulfatrim plus LPS[b]		Sulfatrim plus PIC	
Taxonomy[a]	Prevalence[c]	Abundance[d]	Prevalence[c]	Abundance[d]	Prevalence[c]	Abundance[d]
Actinobacteria	100	0.07	100	0.05	100	**0.09**[e,*]
Bifidobacterium	100	0.03	100	0.02	100	**0.07**[*]
Coriobacteriaceae	100	0.01	100	0.02	100	**0.01**[*]
Enterorhabdus	100	0.02	100	0.01	100	**0.01**[*]
Bacteroidetes	100	71.43	100	68.98	100	**67.21**[**]
Alistipes	100	2.05	100	0.55	100	5.20
Bacteroidales	100	0.04	100	0.07	100	0.03
Bacteroides	100	3.08	100	2.47	100	**3.88**[*]
Parabacteroides	100	0.13	100	0.13	100	**0.05**[***]
Porphyromonadaceae	100	0.15	100	0.14	100	**1.14**[*]
RC9-gut-group	100	0.65	100	0.69	100	**3.23**[***]
Rikenella	100	0.60	100	0.08	100	**0.73**[***]
S24–7	100	57.73	100	65.01	100	47.55
Cyanobacteria	100	0.05	100	0.06	100	**0.15**[*]
4C0d-2	100	0.05	100	0.06	100	**0.15**[*]
Firmicutes	100	21.13	100	23.61	100	28.44
Anaerotruncus	100	0.20	100	0.17	100	0.26
Christensenellaceae	100	0.00	100	0.00	90	0.00
Clostridiales	100	2.42	100	0.60	100	2.20
Coprococcus	100	0.05	100	0.02	100	0.07
Erysipelotrichaceae	100	0.08	60	0.00	100	**0.02**[*]
Sequences/specimen[f]	153,818		145,117		150,759	
Good's coverage (%)	99.99		99.99		99.99	
Genus richness	49.8		44.0		44.5	
Specimens (*n*)	6		5		10	

The numbers in bold represent differences with P values <0.01, <0.05, or <0.1. PIC, poly I:C. [a]Phylogeny of bacterial taxa, assigned by 16S rRNA sequence analysis. [b]The LPS data from MyD88 deficient RIP-B7.1 mice was also included for reference but excluded from statistical analysis. [c]Prevalence (%) of 16S rRNA sequences for bacterial clade and treatment group. [d]Median relative abundance (%) of 16S rRNA sequences for bacterial clade and treatment group. [e]Results of a two-part statistical test of bacterial prevalence and abundance. [f]Median values. *$P < 0.05$, **$P < 0.1$, ***$P < 0.01$, TLR9-deficient mice treated with sulfatrim plus PIC vs. MyD88-deficient mice treated with sulfatrim plus PIC.

and *Bacteroides* in fecal samples from mice on day 5 after the last poly I:C injection. Data shown in Fig. 4*A* confirm and further extend the high-throughput data, indicating that treating TLR9-deficient but not TLR3- and MyD88-deficient mice with sulfatrim plus poly I:C leads to a significant increase in the levels of *Bifidobacterium* and *Lactobacillus* compared with mice that received sulfatrim only ($P < 0.001$ and $P < 0.05$, respectively). Giving sulfatrim plus poly I:C did not modulate the abundance of *Bacteroides* and *Clostridium* in all mouse strains (Fig. 4*A*). Furthermore, samples from all the mice that received sulfatrim alone had a similar abundance of *Bifidobacterium*, *Bacteroides*, and *Lactobacillus* (Fig. 4*A*). Only the level of *Clostridium* was higher in MyD88-deficient compared with TLR9- and TLR3-deficient mice. Similar to the high-throughput sequencing data, mice lacking TLR9 had increased levels of *Bifidobacterium* compared with TLR3- and MyD88-deficient mice after the administration of sulfatrim plus poly I:C (Fig. 4*B*; $P < 0.001$). The levels of *Lactobacillus* and *Clostridium* were also increased in TLR9-deficient compared with TLR3- or MyD88-deficient mice ($P < 0.01$ and $P < 0.05$, respectively). In accordance with the high-throughput data, mice with disrupted MyD88 signaling had an increased abundance of *Bacteroides*. A similar trend toward reduced levels of *Bacteroides* was observed in TLR9- versus TLR3-deficient mice, but this difference did not reach a statistically significant level. In contrast to mice treated with sulfatrim plus poly I:C, the administration of poly I:C alone (without antibiotic treatment) had an increase and a reduction in the levels of *Bacteroides* and *Bifidobacterium*, respectively (Supplementary Table 1). Together, the data validate the trends of changes in the intestinal microbiome detected using the high-throughput approach and lend further support to the hypothesis that alterations in bacterial communities in TLR9-deficient mice may be linked with disease mechanisms.

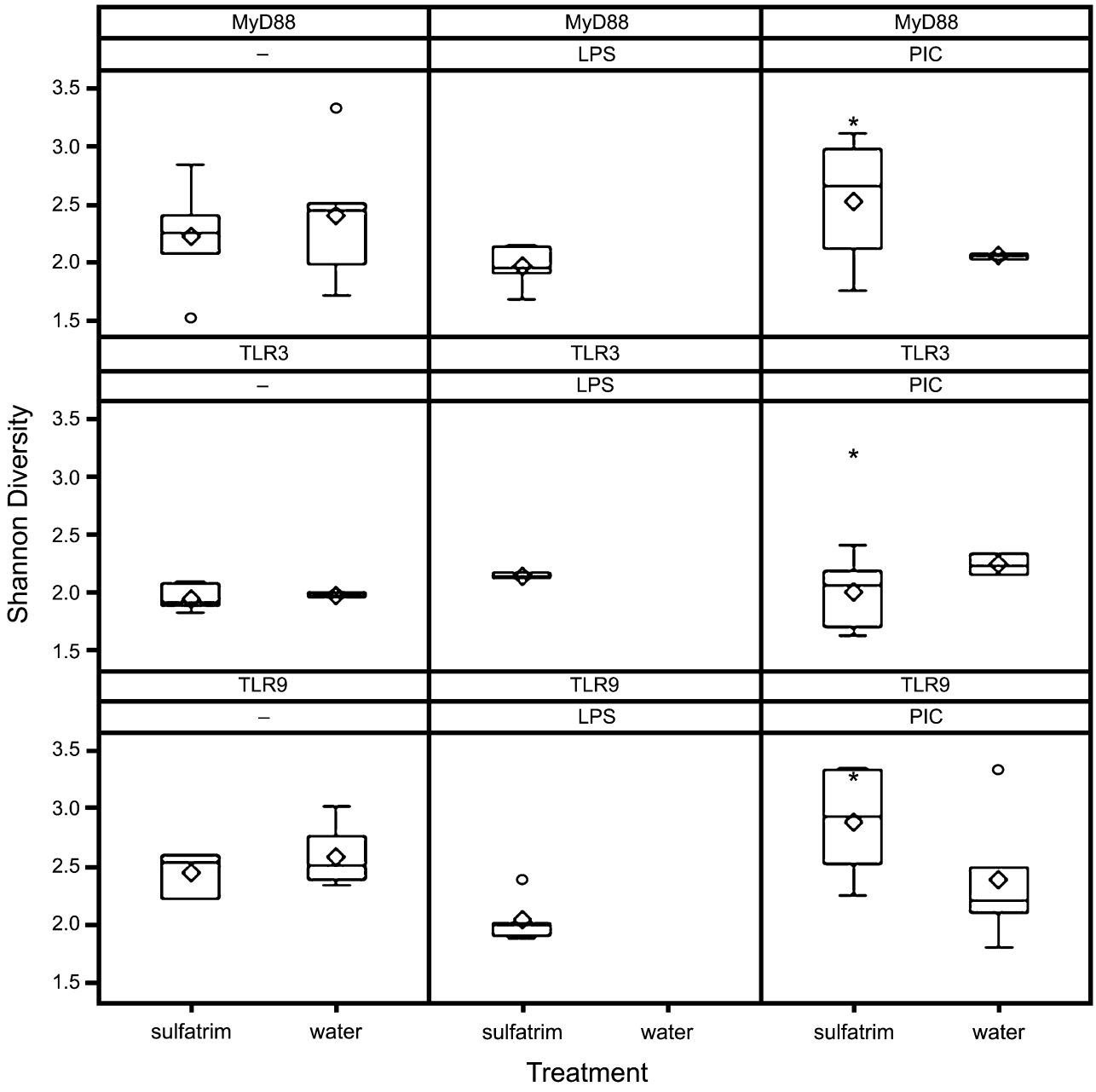

Figure 2—Shannon bacterial diversity in treated vs. untreated mice. The distribution of Shannon indices across animal groups is displayed using box plots. Animals with disrupted TLR signaling received water only or sulfatrim or were treated with sulfatrim plus PIC or sulfatrim plus LPS, as indicated. The area inside the box represents the interquartile range; the median and the mean are denoted by a line and a diamond, respectively. The whiskers extend 1.5 interquartile range from the box, the observations outside of this range are displayed as points. PIC, poly I:C. *P = 0.0002 vs. sulfatrim plus PIC-treated TLR3-deficient mice.

Poly I:C–Induced Serum IL-12/IL-23 p40 in RIP-B7.1 Mice With Disrupted TLR Pathways

We hypothesized that altered cytokine production could be involved in the mechanism leading to diabetes in TLR9-deficient mice. To test this hypothesis, animals were fed with sulfatrim and were intraperitoneally injected with 5 μg/g body weight poly I:C or CpG DNA (n = 3 per group). Peripheral blood was collected 6 h after the treatment, and the serum levels of the p40 subunit of IL-12 and IL-23 was assessed using an ELISA. Data presented in Fig. 5*A* demonstrate that poly I:C administration led to a significant increase in the p40 level in sera from TLR9-deficient mice compared with control untreated animals ($P < 0.001$). Poly I:C injection led to increased p40 levels in TLR3- and MyD88-deficient RIP-B7.1 mice compared with the untreated control; however, these differences did not reach a statistically significant level. Furthermore, the level of poly I:C–induced p40 was substantially greater in sera from TLR9-deficient versus TLR3- and MyD88-deficient animals

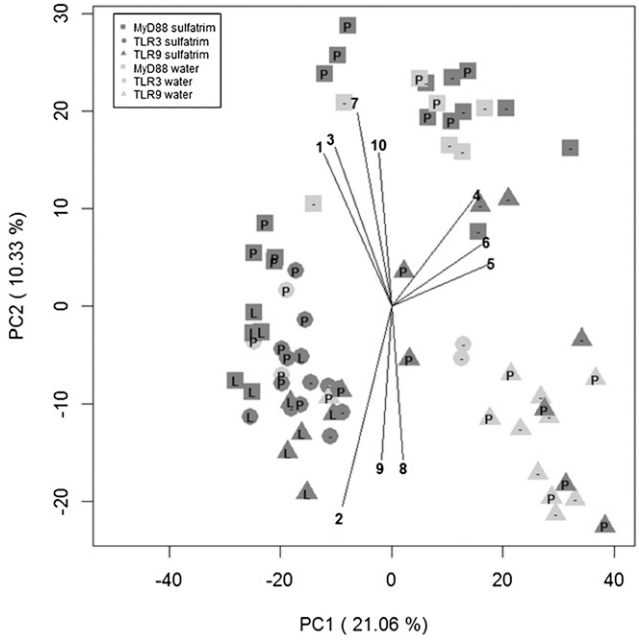

Figure 3—Biplot from the PCA of the intestinal microbiota. The first two principal components (PC1 and PC2) explain 31% of the variability. The PCA scores are displayed for each sample. Animals were treated with sulfatrim with or without poly I:C or LPS, as described in RESEARCH DESIGN AND METHODS. The different shapes correspond to the three different strains. The lighter and darker shades denote treatments with water only and sulfatrim, respectively. Shown on top of the shapes are the treatments added: L (LPS), P (poly I:C), and - (sulfatrim only). Vectors corresponding to the indicated top 10 genera with the highest loadings are displayed. The magnitude and direction correspond to the weights. 1, Porphyromonadaceae; 2, *Odoribacter*; 3, *Rikenella*; 4, *Mucispirillum*; 5, *Leuconostoc*; 6, *Lactococcus*; 7, *Marvinbryantia*; 8, *Ruminococcus*; 9, *Thalassospira*; 10, Desulfovibrionaceae.

($P < 0.001$ vs. TLR3 and MyD88). In contrast to poly I:C administration, the injection of CpG DNA led to a significant increase in the level of the p40 subunit in TLR3-deficient mice ($P < 0.001$ vs. untreated controls); however, as expected, animals with disrupted TLR9 and MyD88 signaling failed to respond to CpG DNA (Fig. 5*B*). Our data indicate that the mechanism of diabetes induction in diabetes-susceptible TLR9-deficient mice may be, at least partially, linked with increased IL-12 or IL-23 production compared with diabetes-resistant TLR3- and MyD88-deficient mice.

DISCUSSION

We have used the RIP-B7.1 mouse model to identify the role of TLR pathways and the gut microbiome in the mechanism leading to diabetes. Our observations suggest that, as expected, the TLR3 pathway plays a critical in the development of poly I:C–induced islet destruction in this mouse; however, activating TLR3 pathways with poly I:C was not sufficient to trigger diabetes. Rather, disrupting the expression of MyD88, which is not involved in mediating poly I:C signaling, also blocked disease induction, suggesting that TLRs other than TLR3 may be linked with the disease course.

Consistent with previously reported findings (14), our data implicate intestinal bacteria in the mechanism protecting the RIP-B7.1 model from disease development. Wen et al. (14) reported that MyD88-deficient NOD mice housed under specific pathogen-free conditions did not develop diabetes. In both the NOD and RIP-B7.1 mice, disease prevention is dependent on the presence of commensal microbes, since housing these mice in a germ-free environment or treating them with sulfatrim (plus poly I:C) resulted in islet destruction (14,27, and this article).

The data imply that TLR pathways have different roles in the NOD versus the RIP-B7.1 mouse model of diabetes. Unlike the NOD mouse, in which disease induction appears to be MyD88-independent (14), MyD88 (and TLR3) signaling pathways play a critical role in islet destruction in the RIP-B7.1 model. The role of MyD88 in disease induction in the RIP-B7.1 mouse model is currently unclear. One explanation is that MyD88 may be involved in sensing tissue damage induced by poly I:C in pancreatic islets or other organs, leading to inflammation and activation of antigen-presenting cells (24). One other difference between the NOD and RIP-B7.1 mouse models is that in contrast to the former model, disease induction in the RIP-B7.1 mouse is TLR9-independent (40). The differences in the roles of TLR pathways in diabetes in these models may be associated with differences related to the mouse strains and mechanisms involved in islet destruction.

Our observations indicate that TLR9-deficient mice had a different intestinal microbiome than that of diabetes-resistant mice. This is based on several lines of

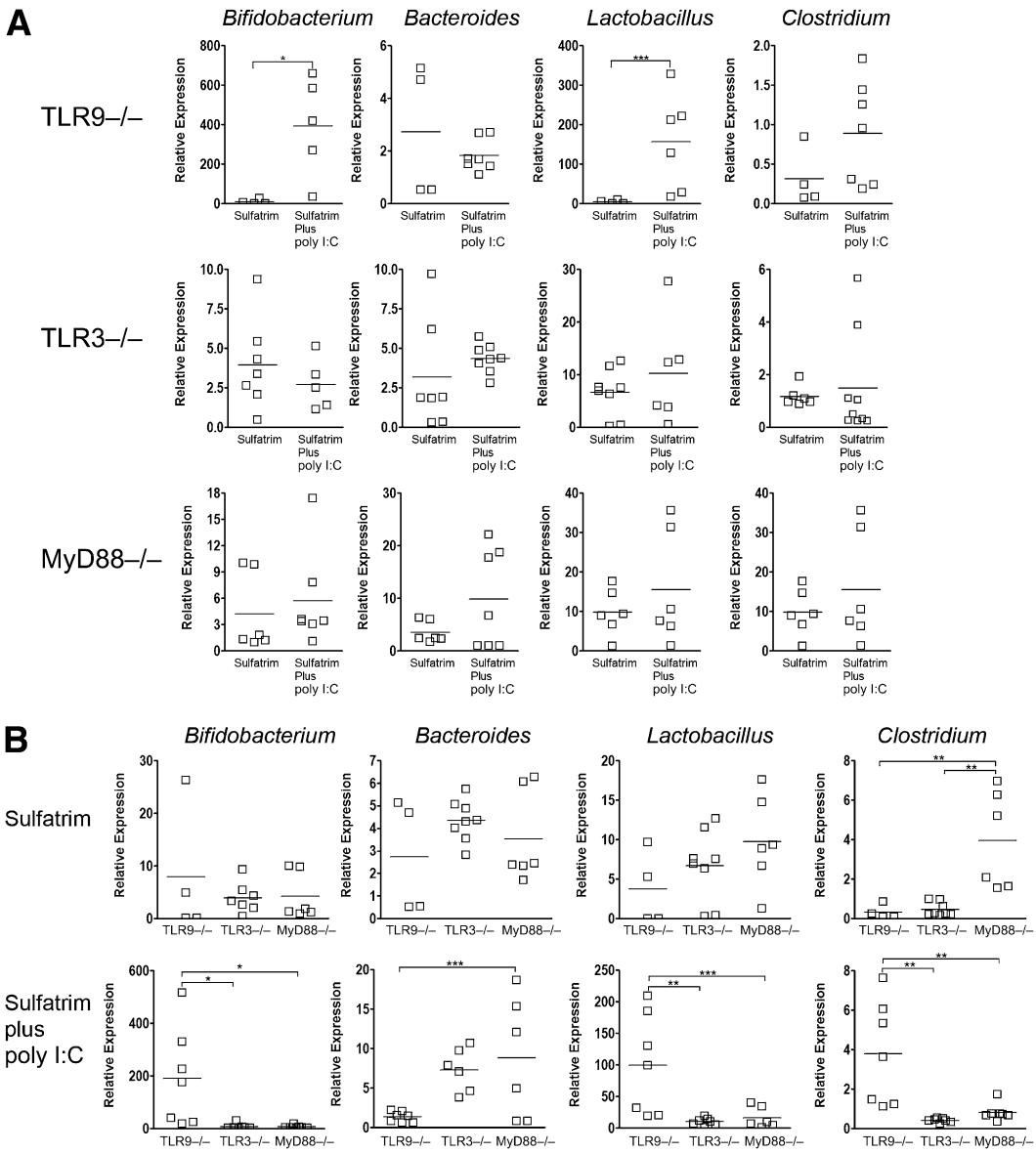

Figure 4—Intestinal bacteria in RIP-B7.1 mice with disrupted TLR signaling. Animals received sulfatrim in the drinking water or were treated with sulfatrim plus poly I:C. DNA was extracted from fecal samples collected from individual RIP-B7.1 mice deficient in TLR9, TLR3, and MyD88, as indicated on day 5 after the last poly I:C injection. Quantitative PCR analysis was used to assess the abundance of bacterial communities, as indicated. Standard curves were obtained using DNA extracted from a fecal sample from a naïve LEW1.WR1 rat. DNA levels were calculated using a bacterial reference gene. Each value represents an individual mouse. *A*: Comparison of bacterial levels from untreated vs. treated animals within each mouse strain. *B*: Comparison between different mouse strains. Bars represent mean values. Statistical analyses were performed using ANOVA with Bonferroni multiple-comparison adjustments. $^{*}P < 0.001$; $^{**}P < 0.01$; $^{***}P < 0.05$.

evidence. First, we found that administering sulfatrim plus poly I:C to TLR9-deficient mice resulted in gut microbiota with higher bacterial diversity compared with TLR3- and MyD88-deficient mice. Second, PCA of the intestinal microbiome indicated that TLR9-deficient mice either untreated or administered sulfatrim plus poly I:C clustered separately from diabetes-resistant mice. In addition, mice lacking TLR9 expression that received sulfatrim plus LPS clustered in the same position as diabetes-resistant TLR3- and MyD88-deficient mice. Third, sulfatrim plus poly I:C modulated the relative abundances of bacteria at the phylum and genus levels. For example, treatment with sulfatrim plus poly I:C led to increased levels of the Actinobacteria phylum and *Bifidobacterium*, *Lactobacillus*, and *Clostridium* genera in TLR9-deficient versus disease-resistant mice.

The finding that sulfatrim plus poly I:C–induced diabetes could be associated with an increase and decrease in the abundance of *Bifidobacterium* and *Bacteroides*, respectively, is in contrast to recent human data, implying that a decrease and an increase in *Bifidobacterium* and *Bacteroides*, respectively, are linked with islet

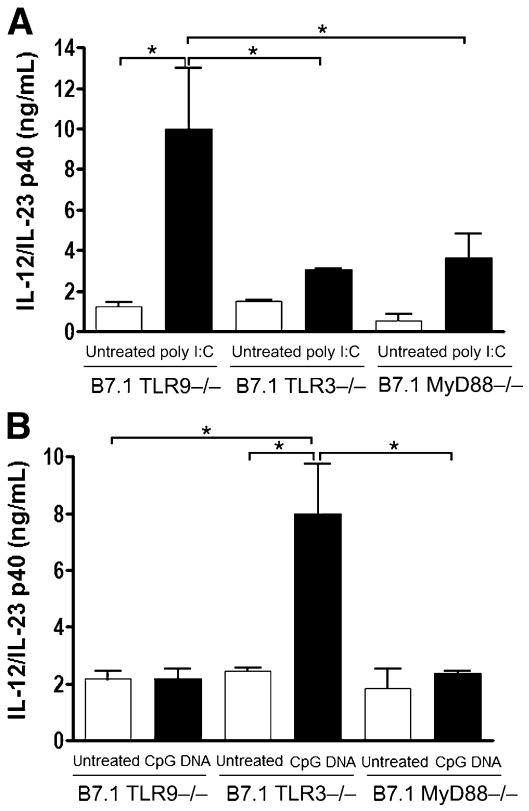

Figure 5—Poly I:C–induced p40 subunit of IL-12 and IL-23 in RIP-B7.1 mice with disrupted TLR pathways. Groups of mice were administered sulfatrim in drinking water beginning at birth (n = 3 per group). Mice were left untreated or were injected with 5 μg/g body weight poly I:C (*A*) or CpG DNA (*B*) at 6–8 weeks of age, as indicated. Peripheral blood was collected 6 h after the injection, and serum p40 levels were determined by ELISA. Statistical comparisons were performed using ANOVA with the Bonferroni multiple-comparison test. Bars represent the mean ± SD. *P < 0.001.

autoimmunity (13,41). However, our observations are compatible with our published data from the LEW1.WR1 rat model that virus-induced T1D is associated with an increased abundance of *Bifidobacterium* (20). Whether and how the altered gut microbiomes identified in genetically susceptible humans or animals are directly linked with T1D are currently unclear. In any case, we suggest that the differences in the potentially disease-promoting bacteria between humans, mice, and rats could be related to the inherent differences between the human and rodent immune systems. They could also be linked with the different timing of the intestinal microbiome analyses with respect to disease onset and progression. Our animal studies were performed early in the course of diabetes, shortly after the administration of the disease trigger, whereas the human studies were performed in samples obtained at a relatively late disease stage after seroconversion.

In contrast to the disease-promoting roles of TLR3 and MyD88 pathways, our results suggest that TLR9 may be involved in mechanisms that attenuate diabetes via an unknown and potentially complex mechanism of action. In light of the important role that gut bacteria play in regulating diabetes in the RIP-B7.1 mouse, it could be that the intestinal microbiome of the wild-type animal confers more resistance to diabetes. We are unable to test this hypothesis because wild-type RIP-B7.1 mice are currently unavailable to us.

Why and how poly I:C triggers diabetes in TLR9-deficient but not MyD88- and TLR3-deficient mice are unclear. One possibility is that poly I:C shifts the balance from anti-inflammatory to proinflammatory gut bacterial composition in mice with disrupted TLR9 signaling. For example, we observed that TLR9-deficient mice had a reduction in the abundance of *Bacteroides*. This effect could theoretically promote a proinflammatory environment, because *Bacteroides* can enhance regulatory T cells and anti-inflammatory cytokine production (42,43). Furthermore, *Bacteroides* can inhibit the activation of the nuclear factor-κB pathway, which is involved in the induction of proinflammatory gene expression (42). We found that among Bacteroidetes, the level of the bacterial family Porphyromonadaceae was increased in diabetes-resistant mice. It is interesting to note that the Porphyromonadaceae sequences were also present at greater abundances in healthy human subjects than in individuals who progressed to T1D (13). Consistent with the possibility that reduced levels of *Bacteroides* may promote proinflammatory responses, we found that higher levels of the p40 subunit of IL-12 and IL-23 were present in the blood from TLR9- versus diabetes-resistant mice shortly after poly I:C administration. It could be that the increase in the level of IL-12 or IL-23 after TLR3 ligation is at least part of the mechanism leading to islet destruction in TLR9-deficient RIP-B7.1 mice. Adding to the complexity, in addition to their immunosuppressive ability, some members of the *Bacteroides* can deliver proinflammatory signals in humans and mice (44). Treatment with sulfatrim and poly I:C also resulted in an increased abundance of *Bifidobacterium* and *Lactobacillus* in TLR9-deficient mice. Many *Bifidobacterium* and *Lactobacillus* strains are known for their anti-inflammatory capability, whereas other bacteria can promote the secretion of proinflammatory cytokines (45–47).

Our data imply that disease development may be linked with altered TLR pathways and gut bacterial communities. How disruption of TLR signaling results in altered gut microbiota in the RIP-B7.1 model is unclear. It was hypothesized that TLR interactions with the commensal microbiota can shape the gut bacterial composition via as-yet-unknown mechanisms (reviewed in Kubinak and Round [48]). Alterations in TLR pathways can prevent certain microorganisms from residing within the intestine. For example, MyD88-deficient mice have a significant increase in the relative abundance of segmented filamentous bacteria in the gut (49). Segmented filamentous bacteria play a fundamental role in the maturation of intestinal T-cell responses (50) and have

been recently implicated in disease prevention in the NOD mouse model (21). Our observations suggest that disease induction in the RIP-B7.1 model may involve interfering with at least two immune pathways. One could be linked with poly I:C–induced activation of the innate immune system triggering the autoimmune attack against pancreatic islets, whereas the other could involve downmodulation of regulatory mechanisms mediated by the intestinal microbiota.

Our data lend support to the hypothesis that the mechanism of sulfatrim and poly I:C–induced islet destruction is dependent on alterations in gut bacterial communities; however, the interpretation of the data should be constrained by the fact that we have not yet established a causal relationship between specific bacteria and disease prevention or induction. Ongoing experiments in our laboratory are designed to identify bacteria that can downmodulate the proinflammatory process, leading to disease onset. It could, however, be that at least part of the mechanism leading to changes in the intestinal microbiota detected after sulfatrim and poly I:C administration are a consequence of the ongoing anti-islet autoimmune process initiated by the treatment regimen. How poly I:C alters commensal bacteria in the gut and how these alterations lead to disease onset requires further investigation.

In conclusion, our data show that TLR3, MyD88, and gut bacteria are critical components in the mechanism leading to poly I:C–induced diabetes in the RIP-B7.1 model. A better understanding of the cross-talk between the innate immune system and gut microbiota early in the disease course could lead to interventions aimed at restoring healthy gut microbial content to prevent islet cell destruction.

Funding. This study was supported in part by grants 1-2006-745, 1-2007-584, 5-2008-224, and 5-2011-41 from the Juvenile Diabetes Research Foundation, and a Diabetes and Endocrinology Research Center Pilot and Feasibility Award (to D.Z.).

Duality of Interest. No potential conflicts of interest relevant to this article were reported.

Author Contributions. A.K.A. maintained the mouse colonies, performed mouse genotyping, and treated animals. N.H. performed mouse genotyping, treated animals, isolated DNA from stool samples, and performed quantitative PCR analyses. E.L. provided the mutated mice and assisted in designing the experiments. D.I. produced the DNA library and performed statistical analyses. C.V.K. conducted the DNA sequencing. C.E.R. and B.D.W. performed bioinformatic analyses. D.N.F. designed and oversaw all aspects of the sequencing experiments and data analysis, researched the data, and participated in writing the manuscript. D.Z. reviewed and analyzed the data, and wrote the manuscript. D.Z. is the guarantor of this work and, as such, had full access to all the data in the study and takes responsibility for the integrity of the data and the accuracy of the data analysis.

Prior Presentation. Parts of this study were presented in abstract form at the 13th International Congress of the Immunology of Diabetes Society, Lorne, Victoria, Australia, 7–11 December 2013.

References

1. Gianani R, Eisenbarth GS. The stages of type 1A diabetes: 2005. Immunol Rev 2005;204:232–249
2. Yoon JW, Jun HS. Viruses in type 1 diabetes: brief review. ILAR J 2004;45:343–348
3. Medzhitov R. Recognition of microorganisms and activation of the immune response. Nature 2007;449:819–826
4. Janeway CA Jr, Medzhitov R. Innate immune recognition. Annu Rev Immunol 2002;20:197–216
5. Chervonsky A. Innate receptors and microbes in induction of autoimmunity. Curr Opin Immunol 2009;21:641–647
6. Wong FS, Wen L. Toll-like receptors and diabetes. Ann N Y Acad Sci 2008;1150:123–132
7. Zipris D. Innate immunity in type 1 diabetes. Diabetes Metab Res Rev 2011;27:824–829
8. Janoff EN, Gustafson C, Frank DN. The world within: living with our microbial guests and guides. Transl Res 2012;160:239–245
9. Round JL, Mazmanian SK. The gut microbiota shapes intestinal immune responses during health and disease. Nat Rev Immunol 2009;9:313–323
10. Cerf-Bensussan N, Gaboriau-Routhiau V. The immune system and the gut microbiota: friends or foes? Nat Rev Immunol 2010;10:735–744
11. Frank DN, St Amand AL, Feldman RA, Boedeker EC, Harpaz N, Pace NR. Molecular-phylogenetic characterization of microbial community imbalances in human inflammatory bowel diseases. Proc Natl Acad Sci USA 2007;104:13780–13785
12. Vaarala O, Atkinson MA, Neu J. The "perfect storm" for type 1 diabetes: the complex interplay between intestinal microbiota, gut permeability, and mucosal immunity. Diabetes 2008;57:2555–2562
13. Giongo A, Gano KA, Crabb DB, et al. Toward defining the autoimmune microbiome for type 1 diabetes. ISME J 2011;5:82–91
14. Wen L, Ley RE, Volchkov PY, et al. Innate immunity and intestinal microbiota in the development of type 1 diabetes. Nature 2008;455:1109–1113
15. Calcinaro F, Dionisi S, Marinaro M, et al. Oral probiotic administration induces interleukin-10 production and prevents spontaneous autoimmune diabetes in the non-obese diabetic mouse. Diabetologia 2005;48:1565–1575
16. Matsuzaki T, Nagata Y, Kado S, et al. Prevention of onset in an insulin-dependent diabetes mellitus model, NOD mice, by oral feeding of Lactobacillus casei. APMIS 1997;105:643–649
17. Brugman S, Klatter FA, Visser JT, et al. Antibiotic treatment partially protects against type 1 diabetes in the Bio-Breeding diabetes-prone rat. Is the gut flora involved in the development of type 1 diabetes? Diabetologia 2006;49:2105–2108
18. Roesch LF, Lorca GL, Casella G, et al. Culture-independent identification of gut bacteria correlated with the onset of diabetes in a rat model. ISME J 2009;3:536–548
19. Lau K, Benitez P, Ardissone A, et al. Inhibition of type 1 diabetes correlated to a Lactobacillus johnsonii N6.2-mediated Th17 bias. J Immunol 2011;186:3538–3546
20. Hara N, Alkanani AK, Ir D, et al. Prevention of virus-induced type 1 diabetes with antibiotic therapy. J Immunol 2012;189:3805–3814
21. Kriegel MA, Sefik E, Hill JA, Wu HJ, Benoist C, Mathis D. Naturally transmitted segmented filamentous bacteria segregate with diabetes

protection in nonobese diabetic mice. Proc Natl Acad Sci USA 2011;108: 11548–11553

22. Guerder S, Picarella DE, Linsley PS, Flavell RA. Costimulator B7-1 confers antigen-presenting-cell function to parenchymal tissue and in conjunction with tumor necrosis factor alpha leads to autoimmunity in transgenic mice. Proc Natl Acad Sci USA 1994;91:5138–5142
23. Devendra D, Jasinski J, Melanitou E, et al. Interferon-alpha as a mediator of polyinosinic:polycytidylic acid-induced type 1 diabetes. Diabetes 2005; 54:2549–2556
24. Wen L, Peng J, Li Z, Wong FS. The effect of innate immunity on autoimmune diabetes and the expression of Toll-like receptors on pancreatic islets. J Immunol 2004;172:3173–3180
25. Kawai T, Akira S. Innate immune recognition of viral infection. Nat Immunol 2006;7:131–137
26. Valladares R, Sankar D, Li N, et al. Lactobacillus johnsonii N6.2 mitigates the development of type 1 diabetes in BB-DP rats. PLoS One 2010;5:e10507
27. Markle JGM, Frank DN, Mortin-Toth S, et al. Sex differences in the gut microbiome drive hormone-dependent regulation of autoimmunity. Science 2013;339:1084–1088
28. Ewing B, Green P. Base-calling of automated sequencer traces using phred. II. Error probabilities. Genome Res 1998;8:186–194
29. Edgar RC, Haas BJ, Clemente JC, Quince C, Knight R. UCHIME improves sensitivity and speed of chimera detection. Bioinformatics 2011;27:2194–2200
30. Schloss PD, Westcott SL. Assessing and improving methods used in operational taxonomic unit-based approaches for 16S rRNA gene sequence analysis. Appl Environ Microbiol 2011;77:3219–3226
31. Pruesse E, Peplies J, Glöckner FO. SINA: accurate high-throughput multiple sequence alignment of ribosomal RNA genes. Bioinformatics 2012;28: 1823–1829
32. Pruesse E, Quast C, Knittel K, et al. SILVA: a comprehensive online resource for quality checked and aligned ribosomal RNA sequence data compatible with ARB. Nucleic Acids Res 2007;35:7188–7196
33. Robertson CE, Harris JK, Wagner BD, et al. Explicet: graphical user interface software for metadata-driven management, analysis and visualization of microbiome data. Bioinformatics 2013;29:3100–3101
34. Jost L. Entropy and diversity. Oikos 2006;113:363–375
35. Aitchinson J. *The Statistical Analysis of Compositional Data*. London, Chapman & Hall, 1986
36. Filzmoser P, Hron K, Reimann C. Univariate statistical analysis of environmental (compositional) data: problems and possibilities. Sci Total Environ 2009;407:6100–6108
37. Alkanani AK, Rewers M, Dong F, Waugh K, Gottlieb PA, Zipris D. Dysregulated Toll-like receptor-induced interleukin-1β and interleukin-6 responses in subjects at risk for the development of type 1 diabetes. Diabetes 2012;61:2525–2533
38. Meyers AJ, Shah RR, Gottlieb PA, Zipris D. Altered Toll-like receptor signaling pathways in human type 1 diabetes. J Mol Med (Berl) 2010;88: 1221–1231
39. Gitlin L, Barchet W, Gilfillan S, et al. Essential role of mda-5 in type I IFN responses to polyriboinosinic:polyribocytidylic acid and encephalomyocarditis picornavirus. Proc Natl Acad Sci USA 2006;103:8459–8464
40. Zhang Y, Lee AS, Shameli A, et al. TLR9 blockade inhibits activation of diabetogenic CD8+ T cells and delays autoimmune diabetes. J Immunol 2010;184:5645–5653
41. de Goffau MC, Luopajarvi K, Knip M, et al. Fecal microbiota composition differs between children with β-cell autoimmunity and those without. Diabetes 2013;62:1238–1244
42. Maynard CL, Elson CO, Hatton RD, Weaver CT. Reciprocal interactions of the intestinal microbiota and immune system. Nature 2012;489:231–241
43. Shen Y, Giardino Torchia ML, Lawson GW, Karp CL, Ashwell JD, Mazmanian SK. Outer membrane vesicles of a human commensal mediate immune regulation and disease protection. Cell Host Microbe 2012;12: 509–520
44. Chervonsky AV. Intestinal commensals: influence on immune system and tolerance to pathogens. Curr Opin Immunol 2012;24:255–260
45. He F, Morita H, Ouwehand AC, et al. Stimulation of the secretion of proinflammatory cytokines by Bifidobacterium strains. Microbiol Immunol 2002;46:781–785
46. He F, Morita H, Hashimoto H, et al. Intestinal Bifidobacterium species induce varying cytokine production. J Allergy Clin Immunol 2002;109: 1035–1036
47. Morita H, He F, Fuse T, et al. Cytokine production by the murine macrophage cell line J774.1 after exposure to lactobacilli. Biosci Biotechnol Biochem 2002;66:1963–1966
48. Kubinak JL, Round JL. Toll-like receptors promote mutually beneficial commensal-host interactions. PLoS Pathog 2012;8:e1002785
49. Larsson E, Tremaroli V, Lee YS, et al. Analysis of gut microbial regulation of host gene expression along the length of the gut and regulation of gut microbial ecology through MyD88. Gut 2012;61:1124–1131
50. Gaboriau-Routhiau V, Rakotobe S, Lécuyer E, et al. The key role of segmented filamentous bacteria in the coordinated maturation of gut helper T cell responses. Immunity 2009;31:677–689